J Electroceram (2006) 17:323–326
DOI 10.1007/s10832-006-0385-0

Photocatalytic property of TiO_2 loaded with SnO_2 nanoparticles

Seung Yong Chai · Young Seok Kim · Wan In Lee

Received: 28 June 2005 / Revised: 10 May 2006 / Accepted: 25 July 2006

Abstract 2.5 nm-sized SnO_2 nanoparticles in rutile phase were loaded on the surface of 25 nm-sized TiO_2 (Degussa P-25) to form SnO_2/TiO_2 nano-composite structure. Up to 10 mol%, the loaded SnO_2 nanoparticles were well-dispersed on the surface of TiO_2 without mutual agglomeration. The SnO_2/TiO_2 with 1 mol% of SnO_2 demonstrated 1.5–1.7 times of photocatalytic activity compared to the pure TiO_2 in decomposing gaseous 2-propanol and in evolving CO_2. The role of SnO_2 nanoparticles on TiO_2 surface is considered to be retardation of recombination rate between electrons and holes by trapping the photo-excited electrons from the conduction band of TiO_2.

Keywords SnO_2 · Nanoparticle · SnO_2/TiO_2 · Photocatalyst

1 Introduction

Variety of strategies has been applied for the improvement of photocatalytic activity of TiO_2 in decomposing organic pollutants [1–3]. So far, the photocatalytic efficiency of TiO_2 has mainly been improved by the loading of some noble metals, such as Au, Ag, Cu, Pd, etc., on its surface [4–8]. In the metal-loaded TiO_2, the recombination between the photoexcited electrons and holes are suppressed, because the electrons on the conduction band of TiO_2 can be trapped to those metal clusters. It was also reported that the efficient photocatalysts can be obtained by the doping or incorporation of some semiconductors such as WO_3 [9, 10], MoO_3 [10], SiO_2 [11], MgO [12], Fe_2O_3 [13], etc., into the lattice or on the surface of the TiO_2. The functions of those metal oxides are complicated, but their main role would be the increase of surface acidity, the generation of defect site, and/or the increase of surface area, etc. Previously, Kamat et al. reported that a high photodegradation rate of organic dye was achieved from a mixture of TiO_2 and SnO_2 colloidal suspensions [14]. Several research groups indicated that the role of SnO_2 is the electron trapping, since the conduction band of SnO_2 is considerably lower than that of TiO_2 [15–20]. Herein, we prepared the quantum-sized SnO_2 nanoparticles junctioned on the surface of TiO_2 (Degussa P25). The structure of SnO_2/TiO_2 was characterized, and its photocatalytic behavior in decomposing gaseous 2-propanol was analyzed.

S. Y. Chai · Y. S. Kim · W. I. Lee (✉)
Department of Chemistry, Inha University, Incheon, 402-751 Korea
e-mail: wanin@inha.ac.kr

2 Experimental

To achieve a junction between 2.5 nm-sized SnO_2 nanoparticles and 25 nm-sized TiO_2 (Degussa P25), the stoichiometric amount of the each powder was mixed in aqueous solution by stirring and sonication. After drying, the mixture was heat-treated at 400°C for 2 h. X-ray powder diffraction patterns for the SnO_2/TiO_2 particles were obtained by using a Rigaku Multiflex diffractometer, with monochromated high-intensity Cu K_α radiation. For the observation of the nanoparticles by TEM (Philips CM30 transmission electron microscope operated a 250 kV), 1 mg of SnO_2/TiO_2 particle was dispersed in 50 mL of water and a drop of suspension was then spread on a holey amorphous carbon film deposited on Ni grid (JEOL Ltd.). UV-visible diffuse reflectance spectra were obtained by a Perkin-Elmer Lambda 40 spectrophotometer.

The prepared SnO_2/TiO_2 samples were tested as photocatalysts for the decomposition of 2-propanol in gas phase. For the photocatalytic measurements the aqueous colloidal

suspensions containing 2.0 mg of SnO_2/TiO_2 were spread as a film form on a 2.5×2.5 cm^2Pyrex glass, and subsequently dried at 50°C for 2 h. The gas reactor system used for this photocatalytic reaction is described elsewhere [10]. The net volume of the gas-tight reactor was 200 mL, and a SnO_2/TiO_2 particulate film was located in the center of the reactor. A 300-W Xe lamp emitting UV and visible light were irradiated to the SnO_2/TiO_2 film through a water filter and the 2-inch diameter silica window on the reactor. After evacuation of the reactor, 1.6$\mu\ell$ of 2-propanol and 3.2$\mu\ell$ of water were added. In the reactor their partial pressures were 2 and 16 Torr, respectively. The total pressure of the reactor was then controlled to 700 Torr by addition of oxygen gas. Under these conditions, 2-propanol and H_2O remained in vapor phase. After irradiation, 0.5 mL of gas sample in the reactor was automatically picked up and sent to a gas chromatograph (Young Lin M600D) by using an autosampling valve system (Valco Instruments Inc. A60). For the detection of CO_2, a methanizer was installed between the GC column outlet and the FID detector.

3 Results and discussion

Figure 1 shows TEM images and XRD patterns of SnO_2 nanoparticles. The SnO_2 nanoparticles are highly monodispersed and mostly spherical shape with 2.5 nm in diameter, and each of them consists of a single grain in rutile phase. Figure 2 shows the TEM images for the 1, 5 and 10 mol% SnO_2-loaded TiO_2. The 2.5 nm-sized clusters identified to SnO_2 nanoparticles were spread uniformly over the surface of the large TiO_2 particles without mutual agglomeration. This suggests the unusually high binding affinity between SnO_2 and TiO_2. The image of the individual nanoclusters junctioned on the surface of TiO_2 was resolved by a high resolution TEM, as shown in Fig. 2–d. The size of cluster was the same as the original SnO_2 nanoparticles, and its fringe pattern with the spacing of 2.64 Å clearly indicates the (101) plane of SnO_2 in rutile phase.

The photocatalytic activities for the SnO_2/TiO_2 samples in various SnO_2 mol% were evaluated to determine the optimum concentration of SnO_2. For this purpose, a film-type sample was prepared by spreading out the suspensions containing 2.0 mg of SnO_2/TiO_2 onto a 2.5 cm$\times$ 2.5 cm sized Pyrex glass. 2-propanol was utilized as a model compound for the photocatalytic decomposition of organic pollutants, since their oxidative decomposition process is simple and well known [10, 21]. 2-propanol is preferentially decomposed to acetone, and finally mineralized to CO_2 and H_2O. Here, the photocatalytic activity was estimated by two ways. First, the decomposition of 2-propanol to acetone was monitored. The amount of the decomposed 2-propanol after 20 min of irradiation was monitored as a function of SnO_2 composition for the several SnO_2/TiO_2 samples, as shown in

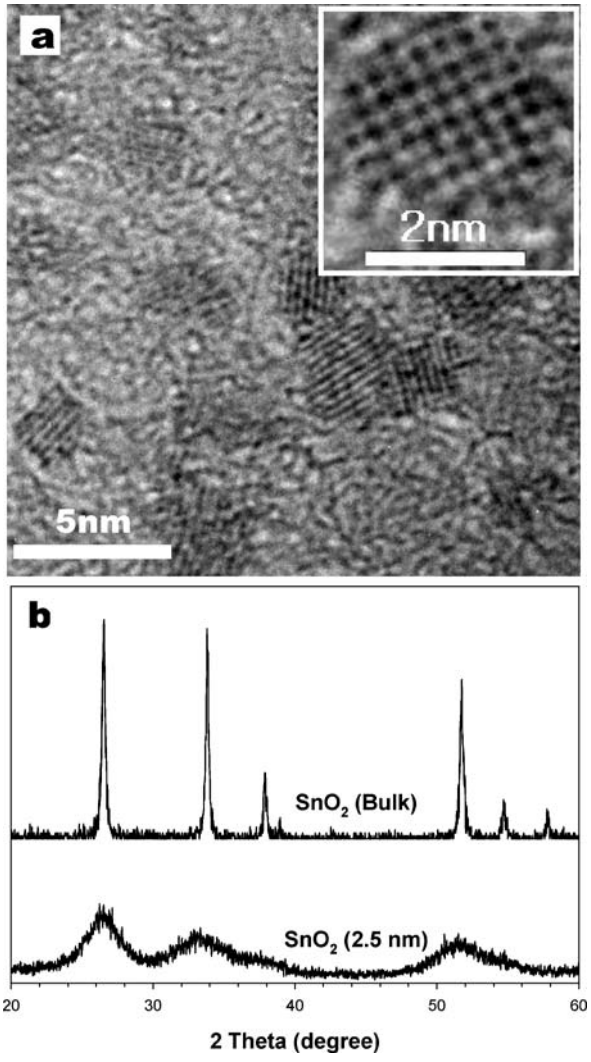

Fig. 1 TEM images (a) and XRD patterns (b) of SnO_2 nanoparticles in 2.5 nm-diameter

Fig. 3(a). 1 mol% SnO_2/ 99 mol% TiO_2 presented the highest photocatalytic efficiency. The decomposed 2-propanol in 20 min of irradiation with 1% SnO_2/TiO_2 was 1.7 times of that with pure TiO_2. Second, the amount of CO_2 evolved as a function of SnO_2 composition was evaluated, as shown in Fig. 3(b). It was also found that the CO_2 evolved with 1% SnO_2/TiO_2 was 1.5 times of that with pure TiO_2.

Diffuse reflectance spectra for the several SnO_2/TiO_2 in different compositions were shown in Fig. 4. The band edge of Degussa P25 with the mixture of 70% anatase and 30% rutile was not appreciably changed by the loading of various amounts of 2.5 nm-sized SnO_2 nanoparticles. This suggests the junction of SnO_2 to the TiO_2 does not modify the band structure of TiO_2.

The band-gap of SnO_2 is 3.8 eV, which is considerably larger than that of TiO_2, whereas the position of the conduction band is lower than that of TiO_2 by 0.5 eV [14]. With formation of the junction between SnO_2 and TiO_2, the

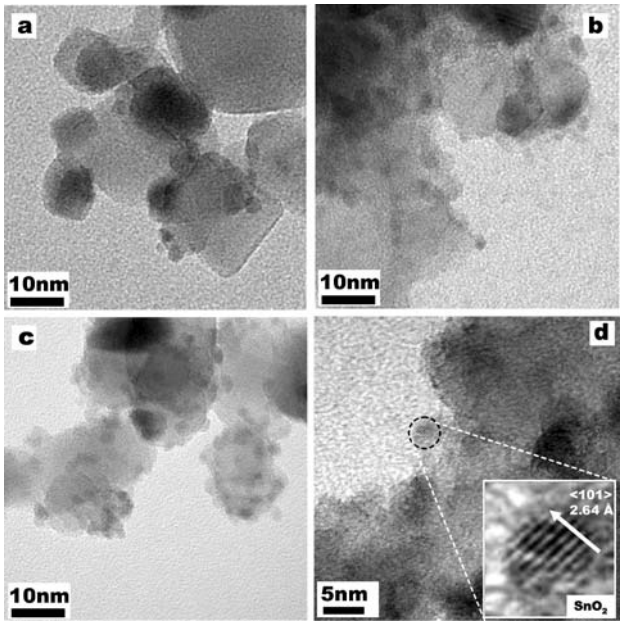

Fig. 2 TEM images of (a) 1 mol%, (b) 5 mol%, (c) 10 mol% SnO_2-loaded TiO_2, and (d) high resolution TEM image for 5 mol% SnO_2-loaded TiO_2

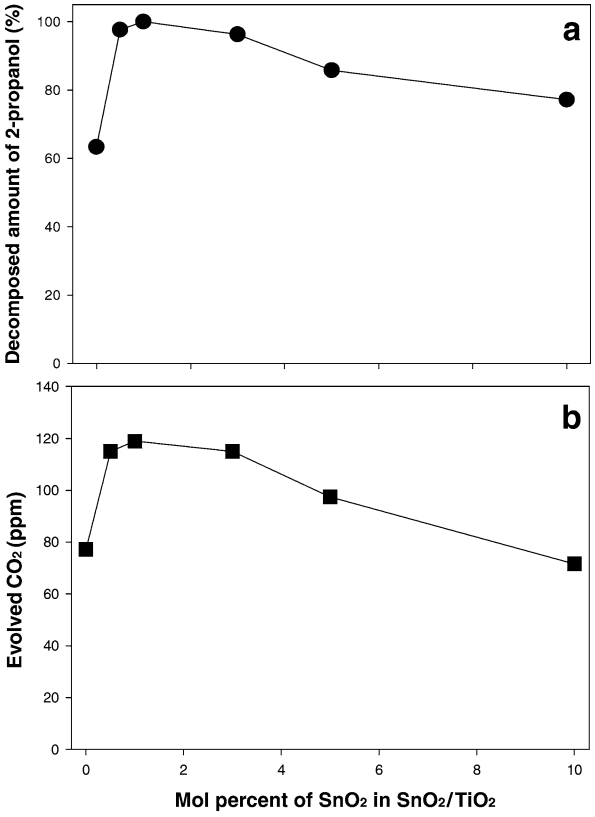

Fig. 3 Decomposition percentages of 2-propanol (a) and the amounts of the evolved CO_2 (b) by photocatalytic reaction as a function of SnO_2 composition in SnO_2/TiO_2 particulate films. For each sample 300 W Xe-lamp was irradiated for 20 min, and the gas compositions in the reactor were 2.0 Torr of 2-propanol, 16 Torr of H_2O, and 682 Torr of O_2

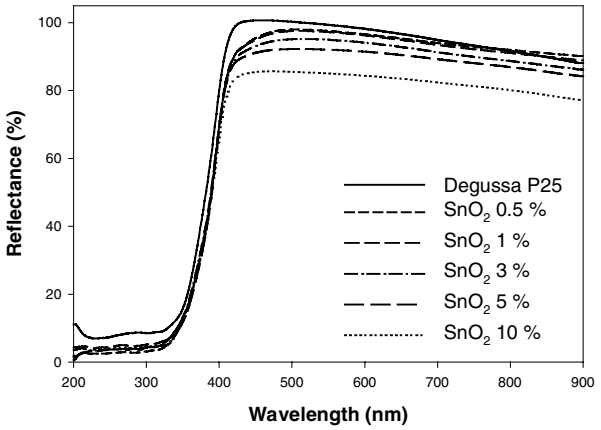

Fig. 4 Diffuse reflectance spectra of SnO_2/TiO_2 powders in different SnO_2 compositions

photoexcited electrons on the conduction band of TiO_2 can be transferred to that of SnO_2 located in considerably lower energy, as proposed by Kamat et al. [14]. With this electron-trapping role of SnO_2, the recombination of electrons and holes in TiO_2 will be suppressed. As a result, more holes on the surface of TiO_2 can participate in the oxidation reaction. The photocatalytic activity was optimized at 1 mol% of SnO_2, and then gradually decreased with further increase of SnO_2 mol%. With a heavy loading of SnO_2 such as 10 mol%, the photocatalytic efficiency was even lower than that of pure TiO_2. This suggests that the SnO_2 itself covering the TiO_2 surface does not work as a photocatalyst, and it blocks some of the catalytically-active site of TiO_2. The role of SnO_2 would be the induction of space-charge separation for the photo-generated electrons and holes of TiO_2, and this role seems to be basically the same as that of noble metals, such as Au, Ag, Pd, etc., loaded on the surface of TiO_2 to improve photocatalytic activity [4–8].

The loading of SnO_2 nanoparticles on the surface of TiO_2 provides several advantages in producing efficient photocatalytic systems, compared with other modifications such as doping or surface loading [15–20]. The SnO_2/TiO_2 junction system can be obtained at a low temperature with high reproducibility, and provides an efficient trapping of electrons, since the highly crystallized SnO_2 nanoparticles possessing clear band structure are applied. In addition, the SnO_2/TiO_2 system is much more stable under an oxidative condition, and costs considerably lower preparation expense, compared with noble metal loaded TiO_2 system. We expect that this process can also be extended to the formation of other junction-type photocatalysts.

4 Conclusions

The SnO_2/TiO_2, prepared by the loading of 2.5 nm-sized SnO_2 nanoparticles on the surface of Degussa P25 TiO_2,

shows the maximized photocatalytic activity at 1 mol% of SnO_2. It shows 1.7 times of photocatalytic activity in decomposing 2-propanol and 1.5 times in evolving CO_2, compared with the pure TiO_2. The role of SnO_2 in enhancing the photocatalytic activity is generating the space-charge separation between the holes in valence band and the electrons in conduction band by trapping the photoexcited electrons from the TiO_2. The quantum-sized SnO_2 nanoparticles are a promising choice for the formation of efficient photocatalytic SnO_2/TiO_2 system.

Acknowledgment This work has been supported by the Korean Science and Engineering Foundation (KOSEF R01-2003-000-10667-0).

References

1. A.J. Nozik, Annu, *Rev. Phys. Chem.*, **29**, 189 (1978)
2. M.R. Hoffmann, *Chem. Rev.*, **95**, 69 (1995)
3. C.S. Turchi, and D.F. Ollis, *J. Catal.*, **122**, 178 (1990)
4. M. Andersson, H. Birkedal, N.R. Franklin, T. Ostomel, S. Boettcher, A. E.C. Palmqvist, and G.D. Stucky, *Chem. Mater.*, **17**, 1409 (2005)
5. A. Kumar and N. Mathur, *Appl. Catal. A*, **275**, 189 (2004)
6. I.H. Tseng, and J.C.-S. Wu, *Catal. Today*, **97**, 113 (2004)
7. A. Di Paola, E. Garcia-Lopez, G. Marci, C. Martin, L. Palmisano, V. Rives, and A.M. Venezia, *Appl. Catal. B*, **48**, 223 (2004)
8. H. Kominami, A. Furusho, S.Y. Murakami, H. Inoue, Y. Kera, and B. Ohtani, *Catal. Lett.*, **76**, 31 (2001)
9. K.Y. Song, M.K. Park, Y.T. Kwon, H.W. Lee, W.J. Chung, and W.I. Lee, *Chem. Mater.*, **13**, 2349 (2001)
10. Y.T. Kwon, K.Y. Song, W.I. Lee, G.J. Choi, and Y.R. Do, *J. Catal.*, **191**, 192 (2000)
11. Z. Ding, X. Hu, G.Q. Lu, P.L. Yue, and P.F. Greenfield, *Langmuir*, **16**, 6216 (2000)
12. J. Bandara, C.C. Hadapangoda, and W.G. Jayasekera, *Appl. Catal. B*, **50**, 83 (2004)
13. M.A. Gondal, A. Hameed, Z.H. Yamani, and A. Suwaiyan, *Chem. Phys. Lett*., **385**, 111 (2004)
14. K. Vinodgopal, I. Bedja, and P.V. Kamat, *Chem. Mater.*, **8**, 2180 (1996)
15. Y. Cao, X. Zang, W. Yang, H. Du, Y. Bai, T. Li, and J. Yao, *Chem. Mater.,* **12**, 3445 (2000)
16. Q. Liu, X. Wu, B. Wang, and Q. Liu, *Mater. Res. Bull*., **37**, 2255 (2002)
17. L.Y. Shi, Y. Zang, D.Y. Fang, C.Z. Li, and H.C. Gu, *J. Mater. Synth. Process*, **7**, 357 (1999)
18. H. Tada, A. Hattori, Y. Tokihisa, K. Imai, N. Tohge, and S. Ito, *J. Phys. Chem., B*, **104**, 4585 (2000)
19. K. Vinogopal, P.V. Kamat, *Environ. Sci. Technol.*, **29**, 841 (1995)
20. J. Yang, D. Li, X. Wang, X.J. Yang, and L.D. Lu, J. *Solid State Chem.*, **165**, 193 (2002)
21. Y. Ohko, K. Hashimoto, and A. Fujishima, *J. Phys. Chem., A*, **101**, 8057 (1997)